

## Development of Formation Flight and Docking Algorithms Using the SPHERES Testbed

Authors: Allen Chen<sup>\*</sup>, Alvar Saenz-Otero<sup>\*\*</sup>, Mark Hilstad<sup>†</sup>, David Miller<sup>‡</sup>

<sup>\*</sup> Graduate Research Assistant, MIT Space Systems Laboratory, 617.253.8541, alchen@mit.edu

<sup>\*\*</sup> Graduate Research Assistant, MIT Space Systems Laboratory, 617.253.8541, alvarso@mit.edu

<sup>†</sup> Graduate Research Assistant, MIT Space Systems Laboratory, 617.258.6872, hilstad@mit.edu

<sup>‡</sup> Director, MIT Space Systems Laboratory, Associate Professor of Aeronautics and Astronautics

**Abstract.** The MIT Space Systems Laboratory is developing the SPHERES formation flight testbed to provide the Air Force and NASA with a long term, replenishable, and upgradable testbed for the validation of high risk metrology, control, and autonomy technologies. These technologies are critical to the operation of distributed satellite and docking missions such as TechSat21, Starlight, Terrestrial Planet Finder, and Orbital Express. To approximate the dynamics encountered by these missions, the testbed consists of three microsattellites, or “spheres,” which can control their relative positions and orientations in six degrees of freedom. The testbed can operate in 2-D on a laboratory platform and in 3-D on NASA’s KC-135 and inside the International Space Station. SPHERES follows the lead of the Laboratory’s MODE (Middeck 0-gravity Dynamics Experiments) and MACE (Middeck Active Control Experiment) family of dynamics and control laboratories (STS-40, 42, 48, 62, 67, MIR, ISS) by providing a cost-effective laboratory with direct astronaut interaction that exploits the micro-gravity conditions of space. Flight tests aboard NASA’s KC-135 have confirmed the functionality of SPHERES as a formation flight test platform with dynamics representative of true spacecraft. Studies in the 2-D laboratory environment include master/slave algorithms and docking control.

### Introduction

The SPHERES (Synchronized Position Hold Engage Re-orient Experimental Satellites) testbed, under development at the MIT Space Systems Laboratory (SSL), provides a cost-effective, long duration, replenishable, and easily reconfigurable platform with representative dynamics for the maturation and validation of metrology, formation flight, and autonomy algorithms. These high risk, yet high payoff control algorithms are applicable to systems requiring coordinated motion of multiple satellites in a micro-gravity environment, including, but not limited to, spare aperture, interferometry, and docking missions. Missions such as the Air Force’s TechSat 21, DARPA’s Orbital Express, and NASA’s Starlight (formerly Space Technology 3) and Terrestrial Planet Finder (TPF), will utilize these algorithms to achieve the capabilities of a single large spacecraft with multiple small separated spacecraft.

The SPHERES testbed allows the testing of (1) relative attitude control and station-keeping between satellites, (2) re-targeting and image plane filling maneuvers, (3) collision avoidance and propellant balancing algorithms, (4) array geometry estimators, and (5) docking control architectures. By operating in micro-gravity, the SPHERES testbed allows algorithm development in a

full 6-DOF dynamic environment resembling those of upcoming missions. Furthermore, the testbed sensors and actuators are traceable to those of real spacecraft. Therefore, the testbed enables the designers of control algorithms to validate the design, initialization, debugging, and refinement process prior to deployment in high cost and high risk missions. The experimental validation of control algorithms and their development processes is an essential step in reducing the considerable risk associated with future formation flight missions.

### **Testbed Overview**

The SPHERES testbed consists of three autonomous micro-“satellites,” a laptop computer, and four small transmitters. It is designed specifically for operation in the shirtsleeve environments of the SSL laboratory, KC-135 reduced gravity airplane, and International Space Station (ISS). The KC-135 and ISS environments provide the ability to test algorithms that may be directly applied to real satellites. The simplicity and hands-on nature of the testbed allow for easy reconfiguration and replenishment of consumables, resulting in low experiment risk and cost. The additional laboratory environment in the SSL enables limited 2-D experiments to be performed before testing on the KC-135 or ISS, reducing even further the cost and risk to develop and verify algorithms.

The SPHERES testbed is designed to produce results traceable to proposed formation flying missions. The individual self-contained satellites have the ability to maneuver in six degrees of freedom, to communicate with each other (satellite to satellite: STS) and with the laptop control station (satellite to ground: STG), and to identify their position with respect to each other and to the experiment reference frame. The laptop control station is used to collect and store data as well as to upload control algorithms to the satellites. Currently, from one to three satellites may be used, depending on the algorithm being tested. The software architecture allows additional SPHERES to be added to the array, if desired. Figure 1 shows an operational concept for the SPHERES testbed, with inter-satellite and satellite-to-laptop interactions illustrated.

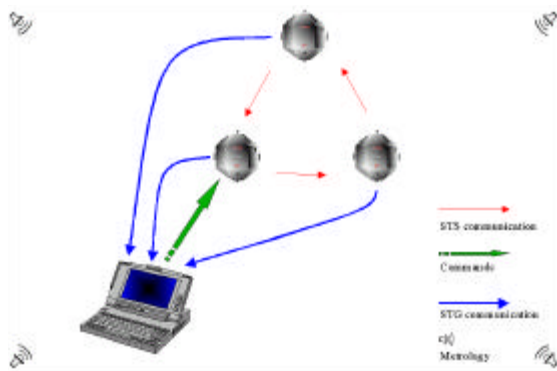


Figure 1. Testbed Operational Concept

### Testbed Description

Each SPHERES satellite contains on-board power, propulsion, processing, radio-frequency communication, and position and attitude determination subsystems. Figure 2 shows a picture of an assembled SPHERES unit floating in the KC-135. An RF interface is attached to the serial port of a standard PC laptop computer, allowing it to function as the ground station. The four external transmitters, also self-contained, use an infrared/ultrasonic time-of-flight range-finding system.

The SPHERES testbed equipment was designed to fit in a Space Shuttle middeck locker, with room for expendables such as propellant tanks and batteries. These space constraints limit the satellite diameter to 0.25 m, about that of a volleyball. Physical properties and other specifications for the satellite units are listed in Table 1.

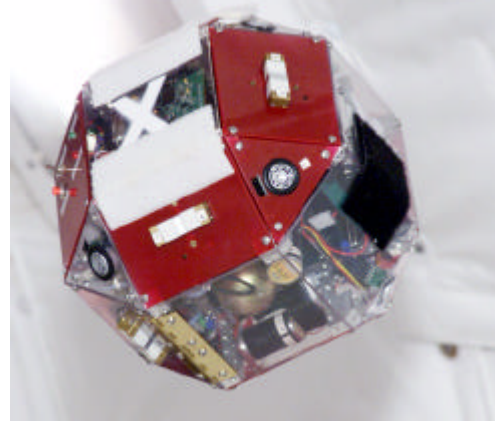


Figure 2. An Assembled SPHERES Unit

Table 1. SPHERES Unit Specifications

Diameter	0.25 m
Mass	3.1 kg
Max Linear Acceleration	0.17 m/s <sup>2</sup>
Max Angular Acceleration	3.5 rad/s <sup>2</sup>
Battery Life	~90 min
Communications Data Rate	19200 kbps
Power	7 W
Metrology Resolution	1.0 cm
Tank Life	~10 min

### Sub-systems Descriptions

The SPHERES subsystems are mounted on an aluminum frame structure, and covered by Lexan panels. The structure was designed using ProEngineer and machined professionally.

The satellites are propelled by a cold-gas thruster system which uses carbon dioxide as fuel. The CO<sub>2</sub> propellant is stored in liquid form at 860 psig, without the need for a cryogenic system. A regulator reduces the pressure to between 20-70 psig; the operating pressure may be adjusted manually prior to each test. A Teflon tubing system distributes the gas to twelve thruster assemblies, grouped in six opposing pairs. The thrusters are positioned so as to provide controllability in six degrees of freedom, enabling both attitude and station keeping control. Each thruster assembly consists of a solenoid-actuated micro-valve with machined nozzles optimized for the desired thrust of 0.25 N. The propulsion system may be easily replenished by replacing a spent propellant tank with a fresh, unused tank.

The Position and Attitude Determination System (PADS) has local and global elements that work together to provide metrology information to the

satellites in real-time. While the global and local elements are capable of independent operation, the readings of both systems are combined during nominal operations to produce continuously updated state information at 50 Hz. The local PADS element provides inertial measurements at 50 Hz, and the global element measurements update those estimates at 1 Hz. The local element consists of three single-axis rate gyros and a three-axis accelerometer. The global element is a GPS-like ranging system that uses ultrasonic time-of-flight measurements from transmitters placed at known locations in the testbed's reference frame to ultrasonic microphones distributed on the surface of each satellite. These time-of-flight measurements are converted to ranges and then used to derive position and attitude with respect to the reference frame.

Each SPHERES unit contains an avionics subsystem which provides electrical power, electronic support hardware, and processing power for the other subsystems.

The power sub-system provides electrical power to the other sub-systems via electronics compatible with the KC-135, Space Shuttle, and ISS. Each satellite utilizes thirteen (13) AA alkaline batteries, which provide a total voltage of 19.5V. This voltage is regulated to 3.3 V, 5 V, 12 V, and 24 V to meet the voltage needs of the different sub-systems. The total power requirement for a SPHERE satellite is approximately 7 W. The demonstrated lifetime of the batteries, during actual operation in both a one-g laboratory environment and the KC-135, is approximately 90 minutes.

Two micro-processors are used in each SPHERES unit. A TIM DIO-40 board manufactured by DSP Systems Inc., based on the Texas Instruments C40 Digital Signal Processing (DSP) chip, was determined the best option for the main software processor. A Motorola 68K processor based board, Onset Technologies' Tattletale 8 (TT8), was selected to support the PADS functions. The decision to use two processors arose from the need for multiple DIO and analog lines in the same system and the need for the PADS system to support several multiple level interrupts asynchronously with the rest of the software system.

The rest of the avionics subsystem consists of a propulsion solenoid driver board, a PADS board, a power distribution board, a UART internal digital communications board, two external RF communications circuits, and eight PADS infrared/ultrasonic receiver boards. The custom boards were designed using OrCAD and procured from professional board manufacturers.

Figure 3 presents the different components of the software architecture. The main components are the controller interrupt, software interrupt, and background processes. The other shown functions are parts of the software architecture that may be exchanged between the different sections of software in order to program the SPHERES testbed with a specific algorithm. This example placement shows how elements of the SPHERES satellite software can work as independent units. The propulsion interrupt operates at 1 kHz, the controller interrupt operates at 50 Hz, and the background processes run freely.

The controller interrupt is considered the main section of the software. The controller interrupt process determines the system state, runs the control algorithm, and determines the necessary output in terms of thruster commands and communication packets. The propulsion interrupt provides the interface to the thrusters, and its rate determines the granularity of the thruster actuation. The interrupt runs at 1 kHz, allowing a pulse width resolution of 1 ms (although the solenoids place a hardware restriction of 5 ms minimum pulse width). The background processes are not time-dependent; they do not need to run at a specific rate. These processes run freely in the background, whenever neither of the interrupts is being processed.

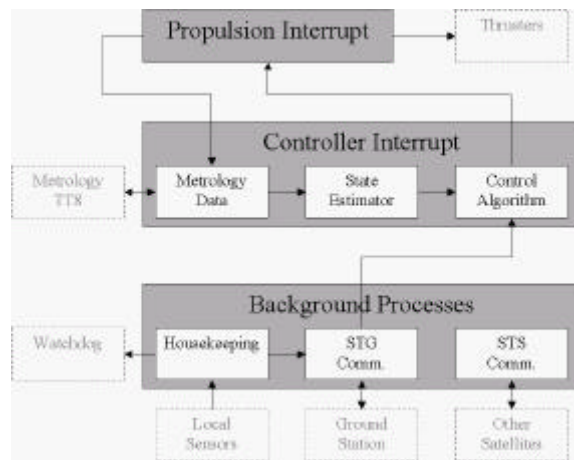


**Figure 3. Software System Designed**

Each SPHERES unit uses two separate frequency communications channels with a data rate of 19.2 kbps. One channel is used for satellite-to-satellite (STS) communications; the other channel enables satellite-to-ground (STG) communications. Both channels are bi-directional; however, the communication hardware is half-duplex, meaning that only one unit can transmit at a time. This requires the implementation of a communications protocol to ensure that only one unit at a time will attempt to communicate, but also that all units are allowed to communicate when necessary. The

developed system utilizes a token ring network that uses packeted data. The token ring protocol ensures that only one unit transmits data at a time. Given the two communication channels, there are two token ring networks: one for the STS network and one for the STG network. The packet format includes the addition of a header with origin, destination, length, and packet type information, plus a tail that contains checksum information. This type of packet allows binary data to be transferred easily, and allows for error detection at the receiving end.

## **TESTING ENVIRONMENTS AND RESULTS**

Development and evaluation of simple formation flight algorithms and of the SPHERES testbed itself have been performed in two distinct environments: aboard NASA's KC-135 reduced gravity aircraft and on a 2-D laboratory air-bearing table. Although KC-135 testing presents some operational difficulties and is limited in duration, it allows testing under the full 6-DOF dynamics, more representative of the spacecraft environment than can be achieved in the laboratory. Consequently, demonstrating the functionality of the testbed through system checkouts and control algorithm testing onboard the KC-135 confirms the usefulness of SPHERES as a formation flight testbed.

The 2-D laboratory environment complements the KC-135 by providing a low cost, tolerant environment, free of time constraints. This environment allows preliminary testing of algorithms in 3-DOF. Furthermore, it is well suited to interactive algorithm development, and for enhancement of the testbed itself prior to deployment in the KC-135 or ISS.

### **KC-135 Flight Tests**

Flight tests of the SPHERES testbed aboard NASA's KC-135 aircraft accomplished two objectives: (1) establish the functionality of the testbed systems and (2) perform limited formation flight experiments. Flight experiments were conducted during one week in February 2000 and one week in March 2000. The time between flights was used to refine operations protocols, improve testbed systems, and develop more complicated experiments using lessons learned from the first week of flights. The flight experiments demonstrated the operability of the SPHERES testbed in a micro-gravity environment.

### ***System Checkouts***

Experiments during the February week of flights concentrated on checkout of all SPHERES systems in a true 6-DOF environment. The propulsion system was

tested using single satellite open loop translational and rotational maneuvers. During these tests, SPHERES team members initialized and released a single satellite in the middle of the testing area during the micro-gravity portion of the parabola. The satellite then executed a predetermined open loop maneuver by firing the appropriate thrusters. Though sometimes unable to overcome the turbulence of the KC-135, the propulsion system provided enough thrust to carry out most desired maneuvers without reaching dangerous speeds. The propellant tanks lasted for an average of ten parabolas, with a pre-programmed maneuver performed during each parabola. The performance of the propulsion system proved adequate for operations of SPHERES as a formation flight and docking testbed.

The PADS system was tested to ensure that its performance could meet the needs of the control algorithms. The local and global elements of the system were tested separately for two reasons: (1) the two elements must be able to operate independently in case of a failure in one element, and (2) an algorithm to combine PADS measurements had not yet been fully developed at the time of the flight experiments.

PADS tests during the first flight week evaluated the performance of the local element, while tests during the second week evaluated the global element. Tests of the local element primarily evaluated the performance of the three rate gyros and the software used to analyze and process the raw data from the gyros. The gyros' accuracy and dynamic range (the maximum and minimum rotation rates that can be detected) were sufficient for the majority of formation flight and docking experiments proposed. Additionally, the gyros proved capable of measuring the high rotation rate of the aircraft's frame during the zero-g trajectory. Operationally, this required initializing the system during the beginning of the zero-g interval, when the aircraft's rotation rate is near constant; otherwise, the airplane frame rotation is interpreted as a large bias by the gyros. The local PADS element provided sufficient accuracy and sensitivity to allow control of all three rotational degrees of freedom.

The global PADS element, which is not affected by frame rotation, was tested during the second week. The global element provided only position fixes, as the software to determine attitude had not yet been fully developed. Laboratory experiments revealed range and field of view limitations of the ultrasound sensors on board each SPHERES unit. The ultrasound sensors were limited to signals within a cone angle of 45° and range less than two meters; consequently, the global PADS software often had insufficient data to determine the position of the SPHERES unit with respect to the

airplane's frame. However, in instances when enough data were present, the global PADS element was able to successfully determine each satellite's 3-D position. The successful solutions showed proof of concept for the global system, while the experimental results have aided in developing better signal processing electronics to detect longer ranges and larger cone angles. These improvements are critical for enhancing the performance of the global PADS element.

The communications subsystem was also tested during flight experiments to ensure that SPHERES could be controlled from the ground station, data from the satellites could be recorded, and the satellites could communicate with one another. All of these tasks are critical to the successful operation of the testbed. Few losses of communications were experienced during free floating maneuvers. Problems encountered were largely due to physical characteristics of the system. The small and delicate antennas used were easily bent out of shape. The fragility of the antennas highlighted the need to replace them with a more sturdy model. Additionally, communications losses usually occurred during initial boots of the SPHERES units; once communications had been established, few interruptions were noted. These startup losses indicated a need to revise the initial synchronization of communications to ensure correct booting.

The SPHERES power system supported nominal operations for in excess of one hour before requiring battery pack replacement. The software system performed as designed; a variety of tests were performed and different maneuver sets commanded via simple commands from the laptop control station. The avionics system also performed as desired, though the tests revealed the need to improve internal wiring to handle greater stresses and fatigue. Finally, the satellite structures proved capable of withstanding both the micro-gravity environment encountered at the top of the parabolas and the high gravity environment experienced at the bottom of the parabolas.

### **Formation Flight Tests**

After validating the functionality of the SPHERES subsystems, simple formation flight tests were performed. These tests demonstrated key formation flight ideas and confirmed that SPHERES is useful as a formation flight testbed. The control scheme tested was based on the master/slave architecture, a very simple form of formation flying control. In this scheme, the state of one satellite, designated the master, is considered the reference state. The master transmits the reference state information to the remaining satellites, dubbed slaves, and each slave determines the actions

necessary to maintain the formation about that reference state. The master/slave tests involved commanding the slave to track the trajectory of the master. The master/slave control scheme allows the formation to be modeled as single unit, simplifying the modeling process. With this simple model, it can be assumed that movement by the master will result in corresponding movement by the slave.

Two types of master/slave architecture tests were performed on the KC-135. In the first, the master was physically attached to the aircraft frame, and the slave was released to float freely near the center of the test area. The slave was given commands to maintain its position and attitude at a constant offset with respect to the state of the master. Disturbances (aircraft rotation and turbulence) forced the slave to perform maneuvers to track the motion of the KC-135. In the second experiment, a test conductor manually rotated the master. The slave was commanded to track and match the master's rotational motion. This scheme was dubbed "joystick" mode, since the master served as the input device to the slave. Joystick mode demonstrated the testbed's ability to perform complex rotation maneuvers while maintaining formation. During these tests PADS and controller state data from the satellites were downlinked to the ground station, while a digital video camera visually recorded test results.

Figure 4 presents results from the first master/slave test, where the master was affixed to the KC-135 frame. Variation in the angle measurements of the master is due to a varying rotation rate of the KC-135 airframe during the micro-gravity portion of a parabola. During these tests, the master unit body coordinates were aligned with the KC-135 frame, with the satellite +X axis pointing towards the right wing (pitch), +Y axis pointing towards the nose of the plane (roll), and +Z axis pointing towards the ceiling (yaw). Test duration was limited to under 15 seconds of micro-gravity due to initial deployment time of the SPHERES units and imperfections in the KC-135 parabolas caused by turbulence and other external disturbances.

Initial deployment is shown in the time period of seconds 442-446. Early deviation of the slave state from that of the master is due to human handling of the slave during deployment. The time period between seconds 446-454 shows the slave closely tracking the master in all three rotational degrees of freedom. The constant angles reported by the master indicate that it is fully tracking the KC-135's motion. After time 454, the trajectories show the KC-135 transitioning out of micro-gravity as the slave is re-captured by test conductors.

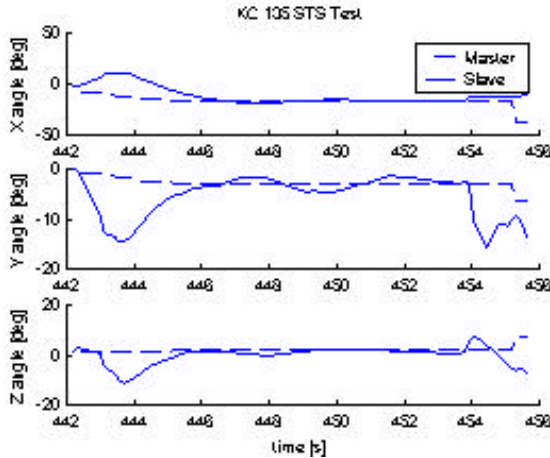


Figure 4. KC-135 airframe tracking experiment.

The Y-axis angle plot in Figure 4 reveals the effects of thruster placement geometry and the asymmetric mass distribution of the SPHERES units. Thruster coupling and the uneven mass distribution produced a low frequency Y-axis oscillation when the satellite attempted to control its X-axis rotation. These effects are only visible in 6-DOF environments.

Telemetry from joystick mode tests is presented in Figure 5. The primary rotation was about the Z-axis; however, master rotations about the X-axis and Y-axis with smaller magnitudes also occurred. The results show that the master z-axis gyro saturated several times during the tests, indicating that the angular rates induced by the test conductor were too high. Although gyro saturation resulted in accumulated error in attitude knowledge, the results do show the slave unit attempting to track the changes in the master unit's state based on the available information.

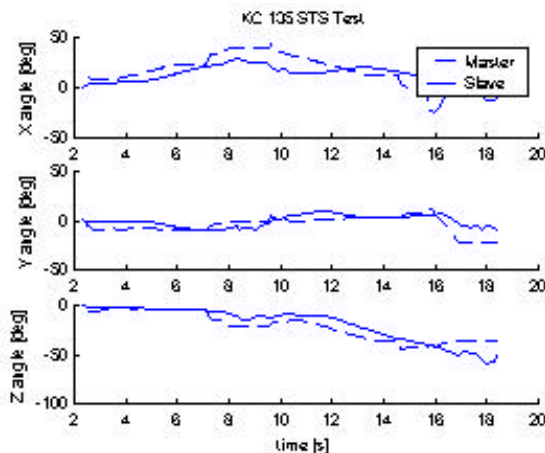


Figure 5. KC-135 6-DOF "joystick" test.

The master/slave tests demonstrated the importance of maneuver anticipation in accurate formation flying control. Due to the nature of the disturbance inputs, the master/slave system was unable to make use of feed-forward techniques, resulting in significant time lag in the slave response. In longer duration tests and in real formation flying applications, the master will autonomously follow a pre-determined trajectory profile, and will do so under its own control authority. The master will therefore be able to communicate upcoming maneuver information to the slaves. This information can be used by the slaves in the calculation of commands based on both the current reference state and the predicted future reference state. This approach will greatly reduce the time lag in the system, and should dramatically improve tracking performance. The illustration of this point is one of the ways that experiments have confirmed the ability of the SPHERES testbed to produce and reveal physically meaningful results and insight.

## 2-D Laboratory Tests

Before and after the KC-135 flight experiments, experiments were performed using an air-bearing table. The laboratory setup provides near-frictionless 2-D motion via carriages that blow air down onto a flat glass surface, a setup opposite that of an air hockey table. The SPHERES satellites mounted to these carriages experience 3-DOF dynamics: two degrees of freedom in translation and one degree of freedom in rotation.

Initial testing using the air-bearing table included four variations of rotation using the master/slave architecture: full state (attitude and attitude rate) 10 Hz, half state (attitude only) 10 Hz, full state 1 Hz, and half state 1 Hz communications. The tests helped evaluate the performance of the SPHERES testbed itself, while providing some insight into the characteristics of master/slave formation flight systems.

Rotations performed during laboratory testing were restricted to rates that do not saturate the propulsion system or rate gyros. This ensures that experiment results provide data useful to the development of formation flight and docking architectures, rather than simply testing the control authority and sensing capability of the SPHERES units. The maneuvers used a "raised cosine" command input. This type of input commands the SPHERES units to follow a continuously varying target trajectory, and eliminates the singularities present in a step or ramp command, where the maneuver profile is not smooth. Figure 6 illustrates the smoothing effect of the raised cosine command versus the sharp corners of a step or ramp command.

The following equation creates a raised cosine path to reach final angle  $\theta_0$  at average rate  $\omega_0$ :

$$\dot{\theta} = \frac{1}{2} \cdot \dot{\theta}_0 \cdot (1 - \cos(t \cdot \dot{\theta}_0 / \dot{\theta}_0)) \quad (1)$$

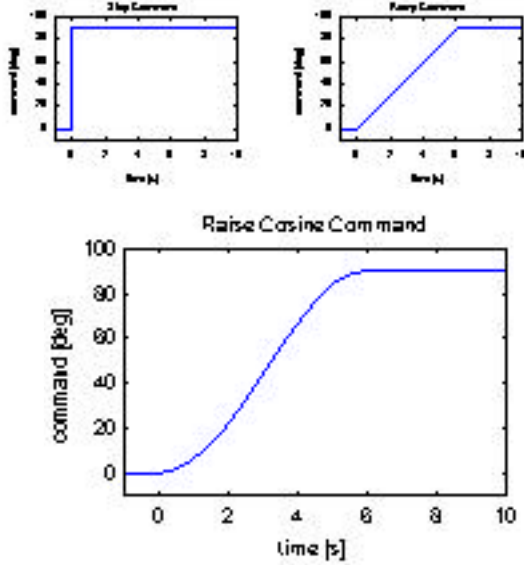


Figure 6. Raised Cosine Reference Input

Initial experimentation with both the model and the testbed showed that for a desired rotation of  $90^\circ$ , an average rate of  $15^\circ/\text{s}$  does not saturate the actuators or rate gyros of the units. As a result,  $15^\circ/\text{s}$  is used for all laboratory experiments.

During the laboratory tests the units are commanded to rotate, following a raised cosine trajectory. No disturbances are intentionally introduced during this path-following phase of the test. The master slew path, therefore, should always closely resemble the raised cosine presented in Figure 6. After the path following, the units are commanded to hold state (prevent rotations). To demonstrate the disturbance rejection characteristics of different control algorithms, the units are disturbed during this time. In order to utilize formation flying systems as virtual rigid bodies, the systems must be able to reject differential disturbances. Figure 7 presents a sample test and illustrates the two test periods.

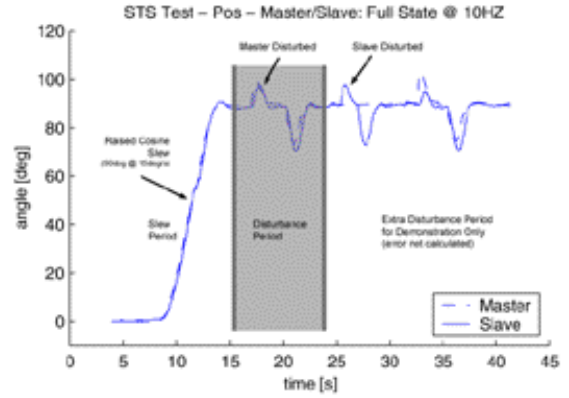


Figure 7. Sample Experimental Run

The errors during the trajectory following maneuver are calculated independently of the errors during the regulation period. These errors are added to calculate the total error for each of the tests. In all cases the presented quantitative errors includes both position and velocity errors, as determined by the following equation for total error:

$$e = \int_{t_1}^{t_3} \left[ \mathbf{a} \cdot (\mathbf{q}_S - \mathbf{q}_M)^2 + \mathbf{b} \cdot (\dot{\mathbf{q}}_S - \dot{\mathbf{q}}_M)^2 \right] dt \quad (2)$$

where  $\mathbf{q}_S$  and  $\mathbf{q}_M$  are the angles of the slave and master units respectively, and  $\dot{\mathbf{q}}_S$  and  $\dot{\mathbf{q}}_M$  are the angular rates. The period  $t_1$  to  $t_2$  corresponds to the start of the rotation maneuver; period  $t_2$  to  $t_3$  corresponds to the disturbance period. The weighting variables  $\mathbf{a}$  and  $\mathbf{b}$  account for the different units, and could be set to penalize errors in angle and rate differently. During

these tests  $\mathbf{a} = \frac{1}{\text{rad}^2}$  and  $\mathbf{b} = \frac{\text{s}^2}{\text{rad}^2}$ .

#### Master/Slave Slews

Two plots of results are provided for each of the laboratory experiments. In each case, the first plot shows the paths followed by the master and the slave, illustrating the overall performance of the system. The second plot shows the calculated error history of each unit throughout each test. The errors for the position and velocity, and their sum for total error, are presented in the same plot.

The plots are followed by a table indicating the integrated error for each test. The total error is the area under the total error curve, determined by integrating the total error curve over the test time period. The slew

error is determined by integrating the error curve during the slew maneuver, but before the disturbance rejection portion of the test. The disturbance error is determined by integrating the error curve throughout the first two responses of the master unit to manually introduced disturbances. Subsequent disturbances are not included in the error calculation. The initial two disturbances of the master unit are sufficient to characterize the performance of the system. The total integrated error will be used as the performance measure.

**Independent Units.** Tests were performed in which two SPHERES satellite units operated independently at the same time. The two units were commanded to follow identical trajectories, but no information was shared between them. These tests were closed-loop from the point of view of each individual satellite, but open-loop from the viewpoint of the formation flying system as a whole. Figure 8 and Figure 9 present the Independent Units architecture angle and error history results, respectively; Table 2 presents the calculated total errors. The plots show the position telemetry data from the master and slave units. The initial slew maneuvers demonstrate the ability of two SPHERES units to carry out the commanded slew. These results show that the expected error of an Independent Units system is minimal when the units are carefully synchronized. The Independent Units configuration does not allow the slave to react to disturbances in the master state (apparent in the disturbance time period), making it unsuitable for applications in which the units are required to behave as a single rigid body in the presence of disturbances. The error due to disturbances constitutes the majority of the total error.

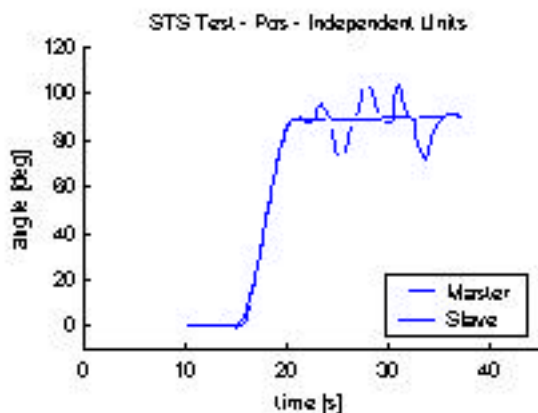


Figure 8. Angular Position for Independent Units

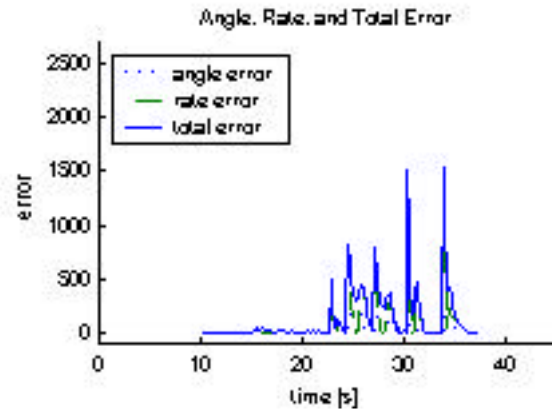


Figure 9. Error of Independent Units

Table 2. Independent Slew Total Error

	Slew	Disturb.	Total
Independent	100	1,907	2,007

**Master/Slave Full State @ 10 Hz.** Figure 10 and Figure 11 present the results of a master/slave formation flying system with 10 Hz communication of the master rotational state (angle and angular rate) to the slave unit. The angle plot in Figure 10 illustrates the approximately rigid body motion of the system when the master is disturbed, as the slave closely tracks the motion of the master. When the slave is disturbed the master does not react; only the slave is concerned with maintaining the relative state and creating dynamics similar to those of a rigid body. This independence of the master behavior from the slave state error is also seen in the Independent Units test.

The errors indicate that the slew maneuver did not perform as well as the Independent Units slews. These results are expected for the case of a fully synchronized independent slew with only minor disturbances (see Figure 8); the master/slave system introduces measurement and communication delays which decrease the performance of the master/slave system. The integrated error in the disturbance period of the master/slave test is approximately half that in the disturbance period of the independent slew. The formation flying algorithm allows the slave to track changes in the master state, reducing the disturbance-induced formation error between the units. The total integrated error is substantially improved in the master/slave (Full State at 10 Hz) test from the independent unit architecture test.

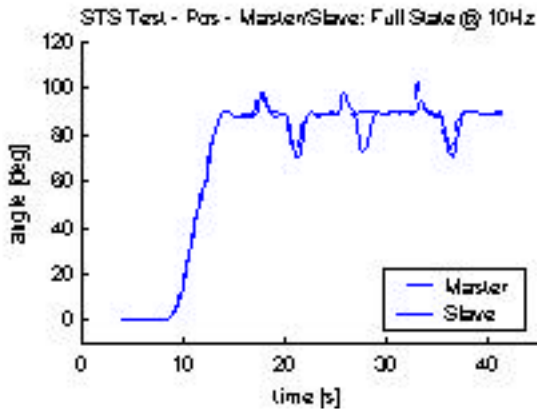


Figure 10. Angular Position for Full State @ 10Hz

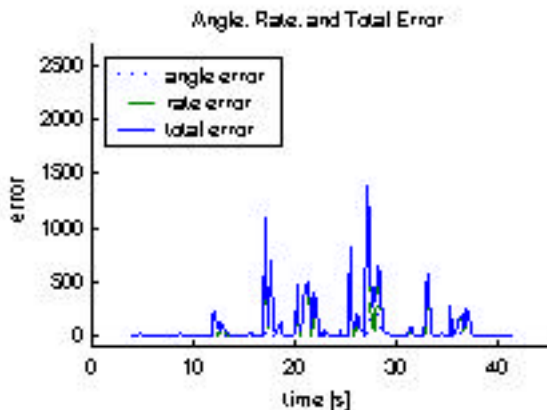


Figure 11. Error of Full State @ 10Hz Test

Table 3. Full State @ 10 Hz Slew Total Error

	Slew	Disturb.	Total
Master/slave	180	1,153	1,333

**Master/Slave Half State @ 10 Hz.** During the half state tests the slave unit utilizes only the angle information in the master reference state; the angular rate of the master is ignored, and the slave desired angular rate is set to zero. Forcing the reference rate to zero increases the damping of the slave response to changes in the master state. The resulting increase in phase lag is illustrated by the increased delay observed in the angle plot in Figure 12. The error for this test is presented in Figure 13.

Table 4 presents the integrated errors for the half state architecture operating at 10 Hz. The error during the slew is more than double that of the Independent Units slews, but the error during the disturbance phase is comparatively small. The total integrated error is lower than that of the independent system. The omission of one half of the master state information does not result

in double the error of the full state test. This behavior demonstrates that formation flying maneuvers are not necessarily dependent on complete knowledge of the master state.

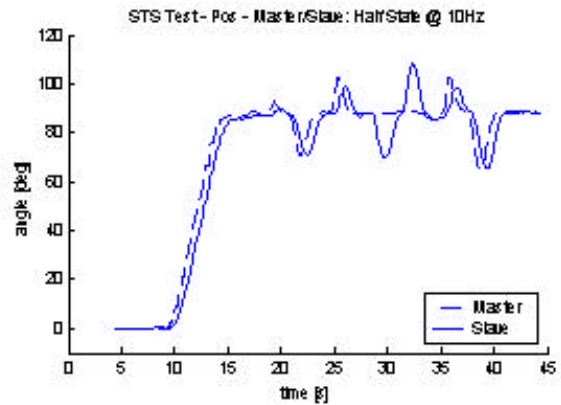


Figure 12. Angular Position for Half State @ 10 Hz

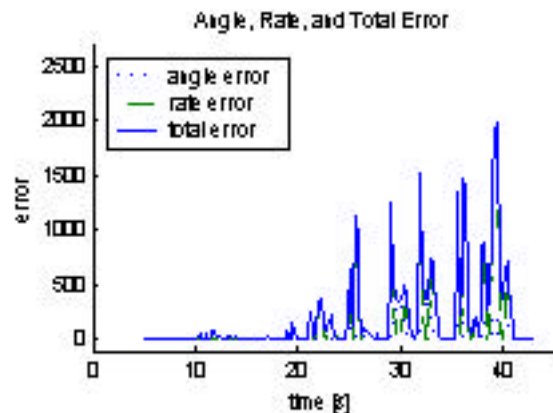


Figure 13. Error of Half State @ 10 Hz Test

Table 4. Half State @ 10 Hz Slew Total Error

	Slew	Disturb.	Total
Master/slave	260	1,432	1,692

**Master/Slave Full State @ 1 Hz.** Figure 14 shows the results on the trajectory of lowering the rate of state transmission to 1 Hz. The slave unit receives the equivalent of incremental step commands during the slew maneuver. Kinks are present throughout the trajectory history, indicating that the slave unit used its maximum thrust between reference updates. During the disturbance maneuver the slave response delay increases substantially. The error plot in Figure 15 shows spikes that hold for longer periods of time than in the previously discussed master/slave tests.

Table 5 presents the integrated errors of the 1 Hz system. The error during the slew maneuver is

substantially larger than in the previous tests. The integrated error during the disturbance test is similar to that seen in the disturbance portion of the Independent Unit test. The total integrated error is 46% higher than with the Independent Unit architecture. This test indicates that the STS transmission rate strongly affects the performance of a master/slave formation flying system.

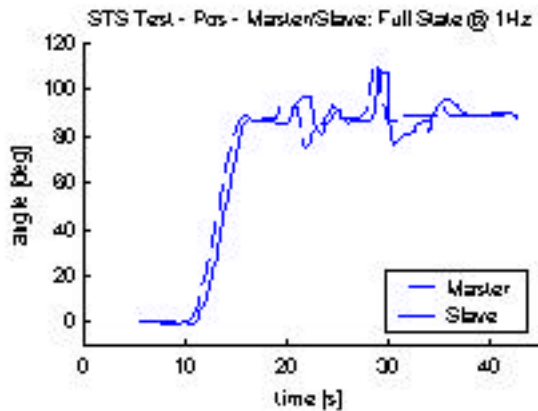


Figure 14. Angular Position for Full State @ 1 Hz

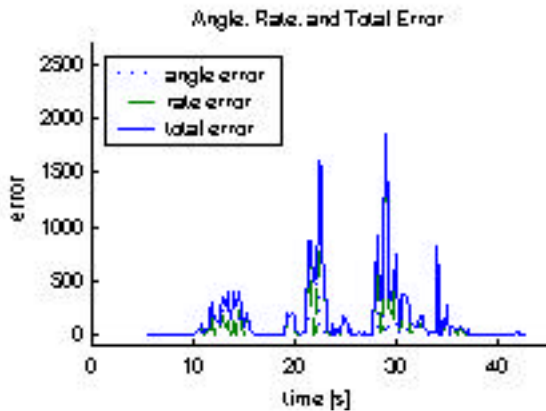


Figure 15. Error of Full State @ 1 Hz Test

Table 5. Full State @ 1 Hz Slew Total Error

	Slew	Disturb.	Total
Master/slave	1,009	1,929	2,938

**Master/Slave Half State @ 1 Hz.** Figure 16 shows the trajectory results for the half state 1 Hz test. The plot shows the effects of the communications delay due to the slow transmission rate, as well as the effect of regulating to zero velocity. The angle of the slave unit is delayed almost two seconds throughout the test; furthermore, it demonstrates the same pulsing motion seen in the results of the full state 1 Hz system. The error plot in Figure 17 shows the large contribution of velocity error to the total error.

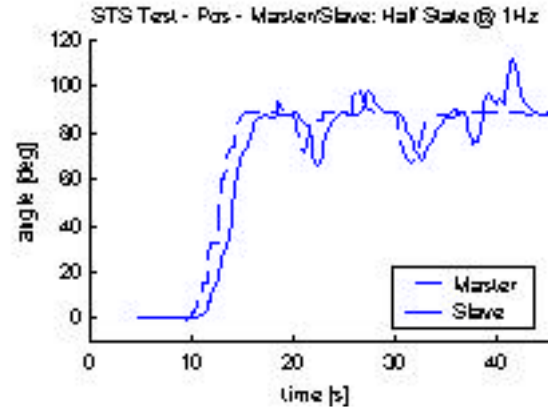


Figure 16. Angular Position for Half State @ 1 Hz

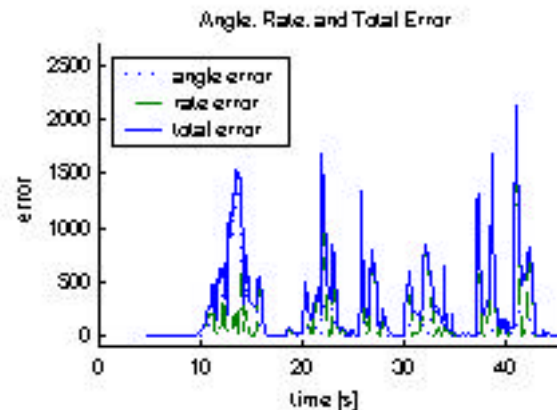


Figure 17. Error for Half State @ 1 Hz Test

Table 6. Half State @ 1 Hz Slew Total Error

	Slew	Disturb.	Total
Master/slave	3,586	1,909	3,495

The total integrated error for this test is shown in Table 6. The total error is nearly double that of the previous test (full state @ 1 Hz); the increase is due to the increased delay during the trajectory-following portion of the test. In contrast, the total integrated error did not increase by nearly a factor of two in the full state case when the rate was decreased from 10 Hz to 1 Hz. This behavior demonstrates the increased effect of reducing the available state information in a 1 Hz system as compared to a 10 Hz system. The importance of a high communication rate is made clear by these results.

**Master/Slave Slew Summary.** The goal of the laboratory tests is two-fold. First, they demonstrate the functionality of the SPHERES testbed. This demonstration includes the ability to implement a formation flying architecture using the SPHERES units, to perform the corresponding autonomous maneuvers, and

to download telemetry data for subsequent analysis. The ability to implement a formation flying architecture demonstrates the capability of the avionics and software systems. Performing autonomous maneuvers proves the functionality of the propulsion, power, and metrology systems. Downloading telemetry data and exchanging state information during formation flying maneuvers demonstrate the functionality of the communications system.

The second goal of the laboratory tests is to obtain an initial understanding of the communications requirements for a formation flying system. For this purpose the experiments used different communications schemes to transmit data between the master and slave units. Table 7 summarizes the results of the five different tests. The tables shows that the Independent Units architecture performs best during the free float maneuver but cannot overcome disturbances. As expected, a reduction of information increases the error; this trend is seen in both the slew and disturbance periods.

**Table 7. Laboratory Results Summary**

Test	Slew	Disturb.	Total
Independent	100	1,907	2,007
Full State 10Hz	180	1,153	1,333
Half State 10Hz	260	1,432	1,692
Full State 1Hz	1,009	1,929	2,938
Half State 1Hz	3,586	1,909	5,495

Table 8 presents the increases in error when changing only one variable (either the amount of transmitted state information or the communications rate). The table separates the increases during the slew (above/right of the diagonal) and the disturbance period (below/left of the diagonal). The least increase in error comes from reducing the amount of state information while maintaining a high update rate. The greatest increase in error comes from reducing the rate from 10 Hz to 1 Hz; both sets of changes confirm this trend.

**Table 8. Percentage Increase in Error During Slew**

State: Rate:	Full 10Hz	Half 10Hz	Full 1Hz	Half 1Hz
Full 10Hz		44%	461%	
Half 10Hz	24%			1279%
Full 1Hz	67%			255%
Half 1Hz		33%	-0.5%	

The experiments indicate that in the development of a formation flying system, emphasis should be placed on attaining the highest possible data rate, even to the extent of reducing variety in the type of state information being sent.

### ***Master/Slave Combined Translation and Rotation***

Building upon flight experiments onboard the KC-135, more complex master/slave formation flight controllers are being developed using the laboratory air table. An enhanced 3-DOF master/slave joystick experiment was developed, where the slave satellite tracks both the position and angle of the master satellite. The coupled translation and rotation of the master satellite makes the slave control task more complex than simply following attitude. As with the other master/slave tests, lag was noticeable. This new test demonstrates the basic functionality of the global PADS system in a formation flying application. While the units are capable of maintaining formation in both relative attitude and position, the precision of the global PADS system must still be improved. Relative position errors were approximately  $\pm 5$  cm; precision of  $\pm 0.5$  cm is desired, and steps are being taken to reduce these errors.

An additional limiting factor in air-table tests involving position is control authority; the slave unit was unable to provide the magnitude of actuation necessary to react to a human moving the master unit. Future work will therefore be based on a master unit undergoing autonomous maneuvers, such that the actuation of both units is comparable.

### ***Docking Architecture Testing***

Autonomous rendezvous and docking experimentation has begun in the 1-g laboratory facilities at the SSL to demonstrate the testbed's ability to perform docking maneuvers. During the 1-g laboratory testing the SPHERES testbed successfully docked two units together. The units performed a cooperative type of rendezvous, meaning that both units can communicate with each other and have actuation capabilities. The master unit held position and orientation, waiting for the slave unit to dock. The two units were controlled via a sub-optimal PD (proportional/derivative) controller.

At the start of the test, the units regulated about their initial positions independently. The initial attitude was pre-set to  $0^\circ$  for the master unit, and  $90^\circ$  for the slave unit. After receiving a start command, the slave unit performed a rotation to point directly at the master. After completing the rotation, the slave then followed a

raised cosine translation trajectory. When the two units were within a few centimeters of each other, the trajectory was updated for the capture stage. In the future a high-precision controller will be used during the capture stage. A docking panel on each unit was fitted with Velcro, and used to secure the units to each other upon contact. The units were not programmed to account for the dynamics of the docked system, so the test terminated as soon as docking occurred.

Figure 18 and Figure 19 shows the results of the docking test. A short movie of the maneuver can be viewed from:

<http://ssl.mit.edu/spheres/darpa/dock.mov>

The first plot of Figure 18 shows the initial conditions of the spacecraft. The second plot shows translation of the slave towards the master, and the resulting positions. The circles in the pictures indicate the outside edges of the SPHERES units; the radius line indicates the orientation of the Velcro docking panel.

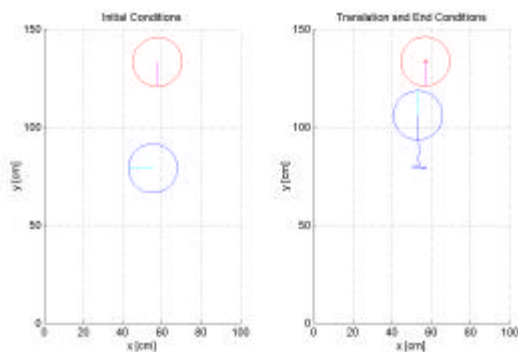


**Figure 18. Position of the Units During Docking**

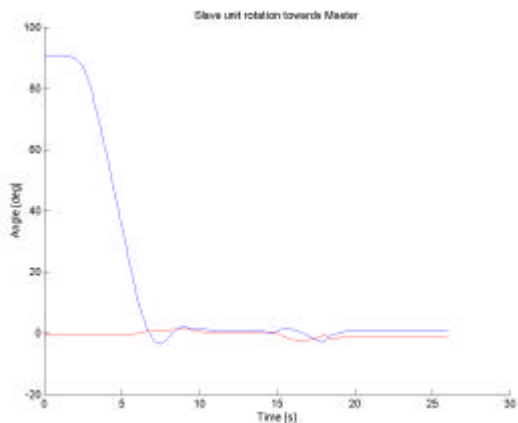


**Figure 19. Angle of the Units During Docking**

The telemetry information from the SPHERES units presented in the figures above illustrates the docking maneuver initial and terminal conditions. As shown in Figure 19, the angles of the two units match very closely, as desired. From Figure 18, however, it appears that the docking maneuver was not performed perfectly. There are slight errors in both the x-direction and the y-direction alignments. This error in the translation is due to the limited accuracy of the current global PADS system. As the video shows, the units did dock. Research is in progress to improve the performance of the global PADS system, as well as to implement more efficient and representative controllers in the SPHERES units to validate the complex docking algorithms. The results described here are encouraging, however, in that they demonstrate the ability of the testbed to execute control algorithms for docking maneuvers.

## Future Work

### Testbed Refinements And Upgrades

Various sub-systems of the testbed are being upgraded to provide better performance, expand experiment options, and comply with NASA manned space flight safety standards. In preparation for operations on the ISS, the satellite structure is being redesigned to provide greater access to the propellant tank, variable pressure regulator, and batteries for servicing. The PADS system has been upgraded with low noise, low drift micro-machined rate gyros. This improvement has led to higher precision attitude determination during long duration tests. Next generation, smaller infrared and ultrasound transmitters and receivers are being incorporated to save use less power, and improve range measurements. A state estimation algorithm using an extended Kalman filter to combine local and global measurements, is projected to significantly improve overall PADS performance. The main microprocessors will be upgraded to a TI C6701 DSP, which provides up to 1 GFLOPS of processing power. The communications system will be upgraded to operate at a 115 kbps data rate using new commercial hardware. To ensure safe operation of SPHERES by astronauts, upgrades include the addition of pressure relief valves, protective sleeves on the batteries, and hardware shutdown controls.

### Optics

Future separated spacecraft interferometry missions, such as NASA's Starlight and Terrestrial Planet Finder, require precise control of optical paths between spacecraft. Interferometric observations require control of optical pathlength difference to a fraction of the

wavelength of light. Because spacecraft are separated by long distances, small errors in beam pointing can create offset errors large enough to break the interferometry beam lock. Requirements on pointing control are therefore very stringent.

To achieve the required pointing and pathlength precision, designs for space interferometry missions utilize a set of staged actuators. Each subsequent actuation stage provides increasing precision, at the expense of a reduction in dynamic range. The coarsest stage is control over the spacecraft relative position and attitude. Spacecraft use thrusters and/or momentum transfer devices such as reaction wheels to reach "ballpark" desired positions and orientations. The finest stage is usually driven by a piezoelectric actuator. This stage has a low range of motion, but high precision and bandwidth. Intermediate stages bridge the gap between the coarsest and finest stages; the stage dynamic ranges usually overlap to ensure smooth transitions and coverage over the range of all expected disturbances. Optimizing the control design of staged actuators for a distributed system presents an important challenge to separated spacecraft interferometers.

To aid in the design of staged control algorithms for separated spacecraft, optical hardware is being developed for installation on the SPHERES testbed. A pen laser, a two-axis piezoelectric-actuated fast steering mirror, and four small solar cells will be added to the SPHERES units. These additional elements comprise the fine stage of a simple two-stage pointing control loop, in which the SPHERES units themselves provide the coarse control. The laser pen source may be fixed to the testbed environment, simulating a fixed target such as a star, or attached to one of the units, similar to a metrology beam. One SPHERES unit will carry the fast steering mirror to redirect the target or metrology beam to another unit, where it will be received by the solar cell array. Using the solar cells as a rough quad-cell sensor, the laser beam can be steered into the center of the cell array, resulting in precise pointing control.

Adding optical hardware to SPHERES makes the testbed an ideal controlled environment for the development of the distributed and staged control algorithms necessary for precision optical control. While less accurate than the interferometry system it mimics, the testbed is also less expensive, less complex, and entails less risk, thus allowing users to achieve a basic understanding of the system without expending large amounts of resources.

## **Formation Flying Algorithms**

The primary goal of the SPHERES project is to provide a development and validation platform for formation flying and docking control algorithms. The simple algorithms tested during the February and March 2000 KC-135 flights successfully verified the basic functionality of the testbed and provided a foundation of experience that has proved useful during continued development of the testbed. Since then, algorithms of increasing complexity have been implemented and evaluated in the laboratory.

As avionics upgrades are completed on the SPHERES satellites, the next step will involve the implementation of advanced algorithms requiring increased processing power and communications bandwidth. A wide variety of optimal control, linear programming, and decentralized control algorithms will be tested in the laboratory, then experimentally validated and comparatively evaluated during on-orbit testing aboard the ISS. Results from these tests will be directly applicable in the design of formation flight missions.

## **CONCLUSION**

Over the past year, flight and laboratory based experiments have confirmed the ability of the SPHERES testbed to produce results relevant to spacecraft formation flight and docking control. Simple master/slave and rudimentary docking scenarios have been explored, while upgrades and refinements to the testbed have increased its capability as the program transitions to operations on the ISS. ISS operation will realize the full potential of the testbed by providing an environment with truly representative dynamics, where long and complex experiments may be conducted. The experiments will have near direct relevance to a number of distributed spacecraft system missions in various stages of development. SPHERES presents an opportunity for formation flight and docking missions to reduce the risk associated with the complex operations of distributed spacecraft. Testing complex control algorithms on a low cost, low risk platform will help ensure mission success.

## **Acknowledgements**

Funding for this research was provided by the Air Force Research Laboratories (AFRL) and by the MIT Department of Aeronautics and Astronautics under the CDIO initiative. The KC-135 flights were sponsored by NASA's Goddard Space Flight Center.

The SPHERES project is the result of a team effort by graduate and undergraduate students and staff of the

Massachusetts Institute of Technology (MIT), with the support of staff from Payload Systems Inc. The project was part of the MIT Department of Aeronautics and Astronautics CDIO initiative, which teaches undergraduate students all the phases of the engineering process: Conceive, Design, Integrate, and Operate. The laboratory class took place during three semesters: Spring 1999, Fall 1999, and Spring 2000.

### **References**

1. Miller, D., et. al., "SPHERES: A Testbed For Long Duration Satellite Formation Flying In Micro-Gravity Conditions", Proceedings of the AAS/AIAA Space Flight Mechanics Meeting, Clearwater, FL, January 2000
2. Saenz-Otero, A., Miller, D. W., "The SPHERES Satellite Formation Flight Testbed: Design and Initial Control", Masters Thesis, MIT Department of Electrical Engineering and Computer Science, Cambridge, MA, August 2000
3. Miller, David W., et al, "SPHERES Design Document", MIT SSL internal document , v2.0, November 1999